UNIVERSITY OF BIRMINGHAM

Research at Birmingham

A Method of Testing Position Independent Geometric Errors in Rotary Axes of a Five-axis Machine Tool Using a Double Ball Bar

Cripps, Robert

[Link to publication on Research at Birmingham portal](#)

A method of testing position independent geometric errors in rotary axes of a five-axis machine tool using a double ball bar

Xiaogeng Jiang, Robert J. Cripps *

School of Mechanical Engineering, University of Birmingham, Edgbaston B15 2TT, United Kingdom

ABSTRACT

Ensuring that a five-axis machine tool is operating within tolerance is critical. However, there are few simple and fast methods to identify whether the machine is in a "usable" condition. This paper investigates the use of the double ball bar (DBB) to identify and characterise the position independent geometric errors (PIGEs) in rotary axes of a five-axis machine tool by establishing new testing paths. The proposed method consists of four tests for two rotary axes; the *A*-axis tests with and without an extension bar and the *C*-axis tests with and without an extension bar. For the tests without an extension bar, position errors embedded in the *A*- and *C*-axes are measured first. Then these position errors can be used in the tests with an extension bar, to obtain the orientation errors in the *A*- and *C*-axes based on the given geometric model. All tests are performed with only one axis moving, thus simplifying the error analysis. The proposed method is implemented on a Hermle C600U five-axis machine tool to validate the approach. The results of the DBB tests show that the new method is a good approach to obtaining the geometric errors in rotary axes, thus can be applied to practical use in assembling processes, maintenance and regular checking of multi-axis CNC machine tools.

1. Introduction

1.1. Background and preliminaries

One of the main criteria for modern manufacturing industry, i.e. aircraft building, mould manufacturing, is the ability to achieve high precision [1]. Due to high accuracy and minimal set-up operations required, five-axis machine tools are thus widely used [2]. Components like impellers are extremely difficult or impossible to machine using 3-axis machine tools but can be easily made by five-axis machines. A five-axis machine tool is generally configured with two rotary axes in addition to the three linear axes. They can be located in the spindle head, in the workpiece side or one rotary axis in the spindle head and one in the workpiece side [3].

However, the rotary axes introduce additional error sources which may lead to flaws and defects in finished components. According to Lei [4], rotary axes are the major error sources in five-axis machine tools. Therefore regular checks and calibration of rotary axes are essential in order to maintain the machine tool accuracy.

Errors existing in multi-axis machine tools are due to flaws in components and joints. They can be broadly classified as

geometric errors, thermally induced errors and dynamic errors. As [2,5] pointed out, geometric errors are the most significant factor affecting a machine's accuracy. Therefore most of the recent research has focused on how to reduce or compensate for geometric errors. According to [6,7], geometric errors of a machine tool can be categorised as position dependent geometric errors (PDGEs) and position independent geometric errors (PIGEs), where "position" is the commanded location of the controlled axis. They are also referred to as component errors and location errors [5,8]. Since the PDGEs are caused by inaccuracies in the machine components and the PIGEs result from the imperfections in the assembly process of the machine components, the value of PDGEs varies from position to position, whilst the PIGEs are constant regardless of the positions of the axes. Much effort has been made to identify and understand PIGEs. In order to simulate these errors mathematically, various models have been developed for both PDGEs and PIGEs [9–11]. The most commonly used method for modelling the PDGEs is to describe them either by *n*th-order polynomials, Fourier or Taylor series [12–14]. Since the PIGEs do not rely on the positions of axes, they can be regarded as constant values [8]. Compared with the PDGEs, PIGEs are easier to determine, thus are examined first [5]. Considering the rotary axes are the major error source, this paper deals with the PIGEs of rotary axes on a tilting-rotary table type five-axis machine tool.

* Corresponding author. Fax: +44 1214144143.
  E-mail address: r.cripps@bham.ac.uk (R.J. Cripps).

1.2. Review on current approaches

A number of methods for testing the accuracy of rotary axes have been proposed recently. Methods included in ISO 230-1:2012 provide a variety of options for testing the geometric accuracy of axes of rotation [6]. The use of an optical polygon with an auto-collimator is able to measure the angular positioning error motion. The combination of a reference indexing table with a laser inter-ferometer/autocollimator is also capable of testing the angular positioning behaviour of a rotary axis. Recently a new commercial product which can be used together with an interferometer to test the positioning accuracy of a rotary axis has been proposed [15]. By having an opposite directional rotation of the retroreflector to the rotary axis under test, the laser beam emitted from the in-terferometer and the one reflected back from the rotary retro-reflector are used as an indication of angular errors. Another ap-plication using a calibration sphere and strain gauge probes pro-vides an accurate health check of rotary axis pivot points [16]. However, these measurement systems are expensive and the setup of the instrument is time consuming. Simple and fast methods are required for checking the rotary axes.

In this study, a DBB has been used to investigate the PIGEs of rotary axes in a five-axis machine tool [17]. A DBB is a piece of one-dimensional length measuring equipment and is ideal for quick checking of 3-axis machine tools. The standard testing scheme comprises three circular tests, namely XY, YZ and ZX planar tests. The DBB software is able to translate the length changes into errors based on the geometry of trace patterns of different individual errors.

In terms of DBB systems used for rotary axes measurement and calibration, previous research initially started from simultaneous movement involving one rotary axis and two linear axes, forming synchronous movements in three different directions [18]. Eight PIGEs were measured using this method. With a few changes in the testing configuration, error conditions of different types of five-axis machine tools can be estimated [19]. The idea of placing the centre of one of the two balls of a DBB on the rotary axis reference straight line has been used by a few researchers, and could simplify the error separation process of the eight PIGEs [8,20,21]. Lei et al. [22] proposed a new trajectory having the *A*- and *C*-axes moving si-multaneously on a tilting rotary table type five-axis machine tool to test the motion errors of the rotary axes performance. An idea of mimicking the cone frustum cutting test using a DBB has been applied to drive all five axes simultaneously [5,23–26].

In terms of minimising the testing time and simplifying the testing procedure, a DBB is an ideal tool for machine diagnostic testing, compared with other methodologies that require longer setup time and greater financial investment [1,2]. However, sim-ple, quick and effective methods using a DBB to test the rotary axes do not exist. This study will focus on the geometric identification and characterisation of the position and orientation PIGEs of rotary axes, in particular the *A*- and *C*-axes, of a tilting rotary type five-axis machine tool using a DBB system. For the purpose of isolating errors from other axes, only one rotary axis is driven and tested in each test. Individual rotary axes were tested by extending the DBB without having to move the centre pivot position. Another ad-vantage of the proposed method lies in its simplicity in fixtures. A standard DBB toolkit can meet the requirement of all test steps. This will enhance the experiment accuracy and reduce the com-plexity of the measurement. The proposed method can also be used on five-axis machine tools with an indexing rotary table having one rotary axis. The following sections outline the ap-proaches to minimise the set-up errors in the spindle tool cup and the centre pivot tool cup. Geometric models are developed to deduce the PIGEs from raw data collected using a DBB. Finally a

brief conclusion is drawn to summarise the contribution of the work.

2. Machine structure and PIGEs of rotary axes

2.1. Five-axis machine tool

As depicted in Fig. 1, a tilting rotary table type five-axis ma-chine tool consists of three linear axes *X*-, *Y*- and *Z*-axes, and two rotary axes *A*- and *C*-axes, which are rotations about the *X*- and *Z*-axes respectively. This type of five-axis machine tool can be seen as a combination of a 3-axis machine tool configured in a standard Cartesian coordinate system and a tilting rotary table.

2.2. PIGEs of rotary axes

According to ISO 230-1 [6], there are five PIGE components for each rotary axis. Fig. 2 shows the PIGEs of the *C*-axis in a 3D co-ordinate system. Corresponding to ISO 230-1 [6], the PIGEs are denoted as the letter "E" followed by a three character subscript where the first character is a letter representing the name of the axis corresponding to the direction of the error, and the second character is a numeral 0 (zero) and the third character is the name of the axis of motion.

There are two linear position errors E_{X0C} and E_{Y0C} in the XY plane, two orientation errors E_{A0C} and E_{B0C} tilting about the *X*- and *Y*-axes and one zero position angular error E_{C0C} for the *C*-axis. If only the position and orientation of the machine tool coordinate system are considered, the zero position error can be ignored [6]. Thus four errors, two position errors and two orientation errors, are needed for identifying the PIGEs for a rotary axis.

The reference straight line in Fig. 2 refers to an associated straight line fitting the measured trajectory of points [6]. It is calculated using least squares, providing a representation of the actual condition of axes [12,13]. Lines 1 and 2 represent the pro-jections of the reference straight line onto the XZ and YZ plane respectively.

Errors in the *A*-axis, shown in Fig. 3, are defined in a similar way. The two position errors are E_{Y0A} and E_{Z0A} in YOZ plane and the two orientation errors are E_{B0A} and E_{C0A}, which are the rotations about the *Y*- and *Z*-axes respectively. Lines 1 and 2 are the pro-jections of the reference straight line onto the XY and XZ planes respectively.
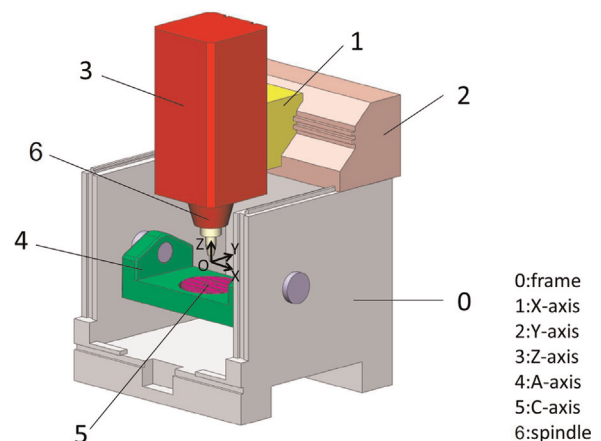

Fig. 1. The structure of a tilting rotary table type five-axis machine tool.
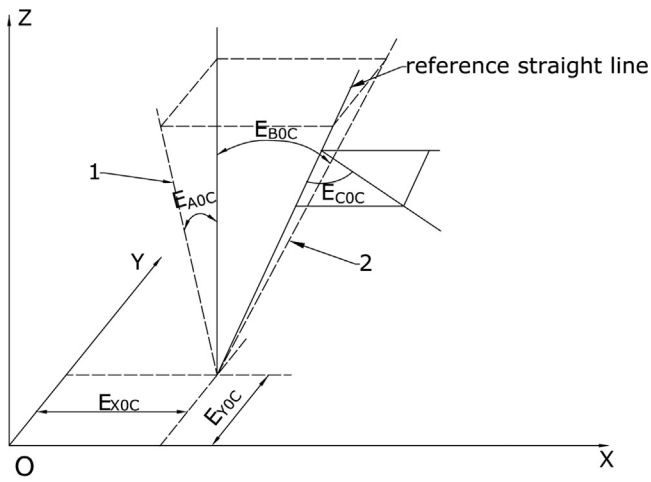
Fig. 2. PIGEs of the *C*-axis.
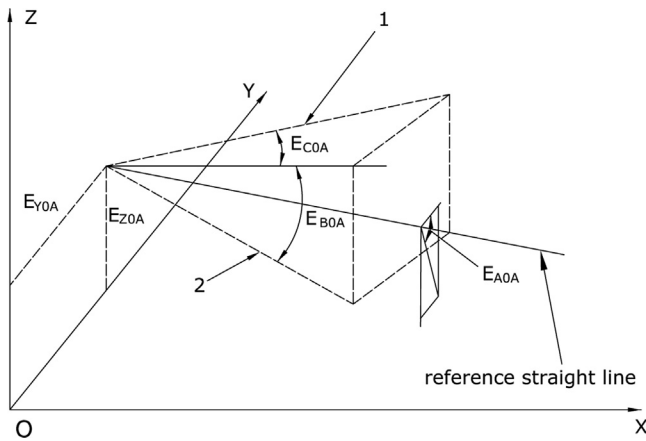

Fig. 3. PIGEs of the *A*-axis.

3. Rotary axes tests

The majority of five-axis machine tools with a tilting rotary table are configured with the *C*-axis rotary table above the *A*- or *B*-axis tilting table [27]. The idea of testing the rotary axes in this paper is to isolate the position and orientation errors and measure them separately. With the assumption that the *X*-, *Y*- and *Z*-axes are within tolerance and hence will not introduce any significant errors, the four procedures of tests are shown in Fig. 4.

3.1. Test set-up

Before discussing the set-up, the reference coordinate needs to be defined. The origin of the reference coordinate system is defined as the intersection of the ideal *A*- and *C*-axes when they are at their zero positions. The three axes of the reference coordinate system are parallel to the three linear axes *X*, *Y* and *Z* of the machine tool coordinate system. First the pivot is attached to the *A*-axis tilting table away from the origin of the reference coordinate system *O*. The centre of the spindle tool cup is then aligned with the *A*-axis. The two balls of the DBB, namely the spindle ball and the table ball, are attached to the spindle and pivot tool cups respectively. This configuration ensures any error captured is caused by the misalignment between the reference straight line of the *A*-axis and its ideal position. Also, since the centre of the spindle tool cup lies on the ideal *A*-axis in the trajectory plane, orientation errors do not have any significant impact on the result, which

means the analysed errors are purely the position errors of the *A*-axis. In order to avoid any collision of the DBB and the machine tool, the *A*-axis tilting movement is restricted to −20° to +70°.

To fit the 150 mm DBB with an extension bar, a displacement of the spindle tool cup in the negative *X*-axis direction is applied (Fig. 4(b)). The same tilting angle of the *A*-axis from −20° to +70° is applied and the trajectory of the DBB is a quarter of a conic surface.

The third step is carried out for the purpose of testing the *C*-axis position errors. Unlike the *A*-axis tests, the *C*-axis rotary table is able to be driven through 360° with the DBB. The centre of the spindle tool cup is set to be at the origin of the reference co-ordinate system. The pivot is placed away from the *C*-axis by a DBB nominal length in the X direction of the reference coordinate system. This ensures only the position errors will be reflected in the result, without any influence from the orientation errors of *C*-axis. However, as the *C*-axis rotary table is on top of the *A*-axis table, position errors in the *Y*-axis direction of *A*-axis will affect the accuracy of the *C*-axis. So the testing results of the *A*-axis should be removed from the errors of the *C*-axis.

In the final step, the orientation errors in the *C*-axis are tested with the same extended DBB. Similar to the idea of testing the *A*-axis orientation errors, the DBB rotates in a full circle with its axis tilted.

3.2. Error elimination before start

The raw data, which is the length changes of the DBB, needs to be converted into coordinate values in the corresponding local coordinate frames for later use. However two error sources appear which affect the accuracy of the test. One is the set-up precision of the spindle tool cup and the other is the position of the pivot tool cup. To ensure the spindle tool cup centre line aligns with the main spindle axis, a dial gauge with a magnetic base mounted on the machine table is used to keep the runout in the horizontal plane within the machine tolerance, which is 1 μm. The spindle tool cup is clamped in the spindle tool holder after the horizontal accuracy is adjusted to the machine tolerance. The centre of the spindle tool cup is then measured in the Z direction with respect to the *Z*-axis zero point with a tool setting probe attached on the table. The test datum is set using the measured spindle tool cup position.

The position accuracy of the centre pivot is obtained by using a planar circular DBB test around the pivot tool cup centre. The *C*-axis set-up procedures are taken as an example to show the process of eliminating the starting position errors. Errors in the placement of the pivot in the Y or X direction will influence the precision since the deviations are in the error sensitive directions [18].

Let P_0 be the ideal start position and P'_0 the actual start position. An error of the rotational angle δ_e will occur (Fig. 5), and is given by

$$\delta_e = \tan^{-1}\left(\frac{\mathbf{P_0P'_0} \cdot \mathbf{j}}{\mathbf{P_0P'_0} \cdot \mathbf{i} + 100}\right) \tag{1}$$

where $\mathbf{P_0P'_0}$ is the vector from P_0 to P'_0, $\mathbf{i}$ and $\mathbf{j}$ are the unit vectors of the *X*- and *Y*-axes respectively, and 100 is the nominal radius of the DBB table ball trajectory.

The vector $\mathbf{P_0P'_0}$ is determined by performing a conventional XY planar circular test around the starting position. These centre offsets are then used to correct the actual starting position P'_0. A similar strategy can be applied to the *A*-axis for the elimination of the start position error. For the *A*-axis start error correction, a partial arc test in the YZ plane is performed after set-up to derive centre offsets in the *Y*- and *Z*-axes directions.
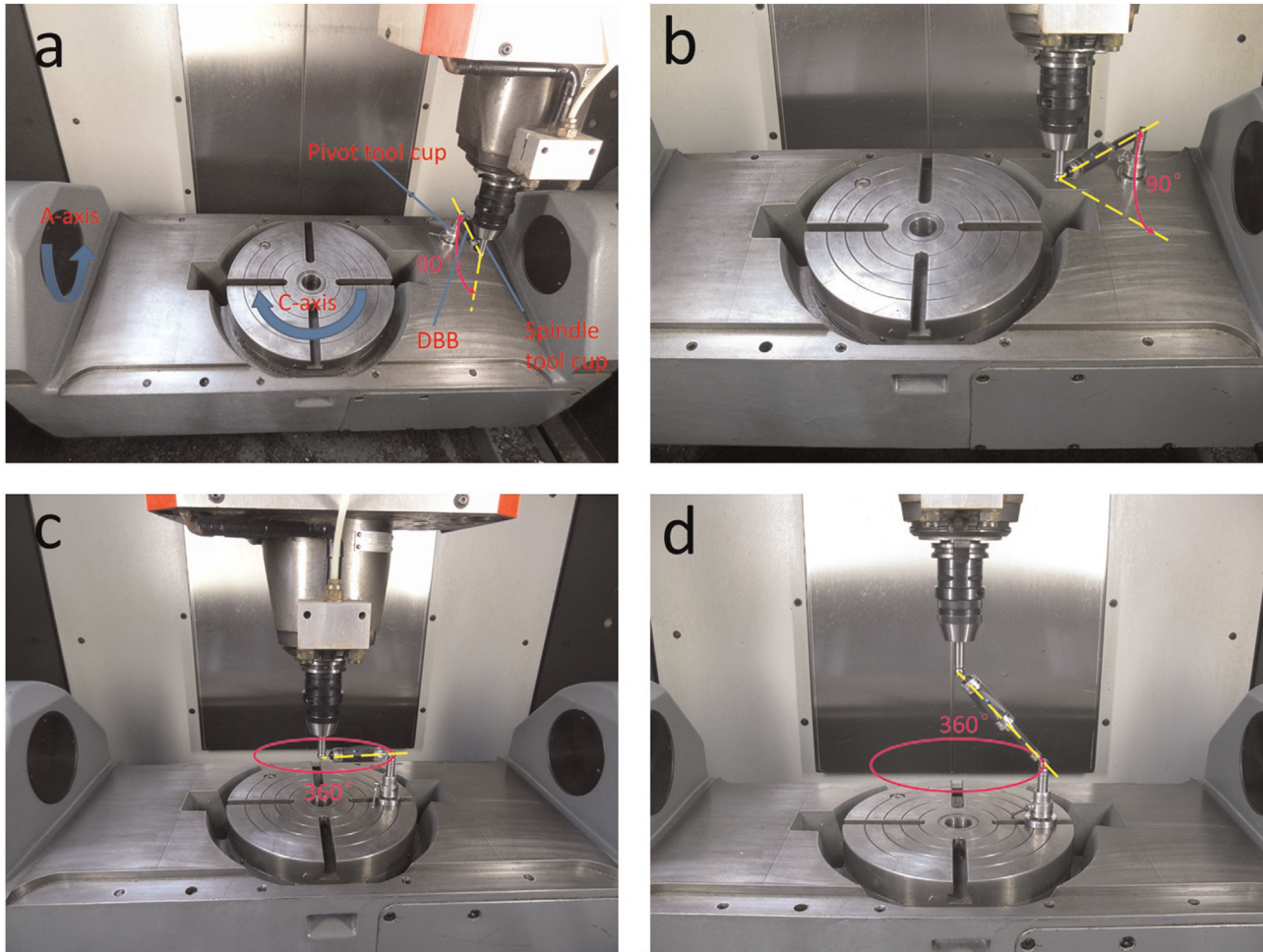
Fig. 4. 4 stage rotary axes test set-up on a five-axis machine tool. (a) *A*-axis test without an extension bar. (b) *A*-axis test with an extension bar. (c) *C*-axis test without an extension bar. (d) *C*-axis test with an extension bar.
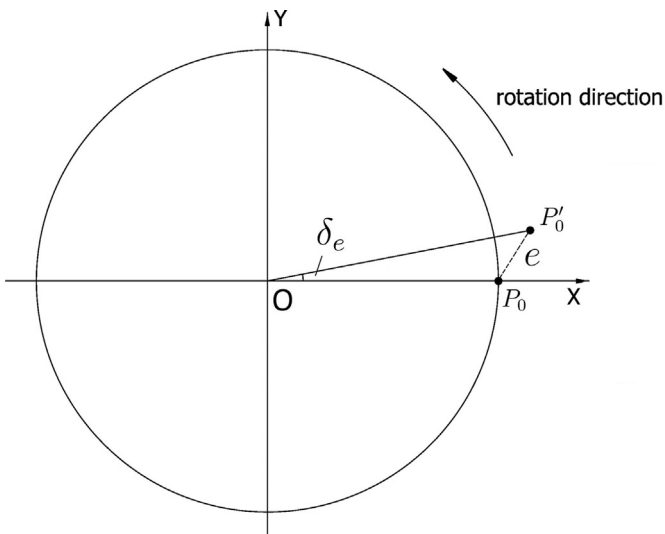

Fig. 5. Influence of inaccurate start position.

3.3. Tests without an extension bar

For tests with and without an extension bar, the processes of modelling and analysing the errors are different. However, the analysis for the same type of test (with or without the extension bar) of different axes is similar, hence the following method can be applied to both axes. Here the *A*-axis is chosen to illustrate the derivation of position errors. For the *C*-axis test without an extension bar (Fig. 4(c)), the method is also valid by simply changing the testing plane from YZ to XY.

The first step (Fig. 4(a)) indicates a 90° movement of the DBB. The measured data of the DBB is the distances between the balls' positions at the spindle and the pivot tool cups. As the DBB trajectory, formed by the two balls, stays in a plane, a planar circular test is established. The DBB trajectory is centre offset from its nominal centre due to the impact of the position and orientation PIGEs. Those errors can be separated once the orientation PIGEs are determined as explained in Section 3.4. However, for consistency reasons, the position errors detected in this step need to be converted to the reference coordinate system. Since the plane that the DBB sweeps has a displacement from the origin of the reference coordinate frame {*O*}, the position errors detected are with respect to the local coordinate system, whose origin is the spindle tool cup centre and the *X*-, *Y*- and *Z*-axes are parallel to those of the reference coordinate system.

In order to obtain the position errors, a mathematical model is proposed. The table tilts about the actual *A*-axis which has a displacement from the ideal *A*-axis. Since the DBB readings are based on the centre of the spindle ball, which lies on the ideal *A*-axis, the centre offset of the DBB readings can be seen as the misalignment between the actual and ideal *A*-axis. Therefore one way of calculating them is to use coordinate transformations. The implied risk

of using such method may cause a distortion in plotting, usually an ovalised shape. However, it has been reported that for eccentricities less than 100 µm, the error is less than 0.2 µm, which is smaller than the desired tolerance (1 µm) [28]. Therefore, any such distortions will be insignificant. Before carrying out the experiment, a measurement using a dial indicator assures the misalignment is less than 100 µm. Therefore, in this paper the coordinate transformation method is employed for calculating the misalignment.

Considering the magnitudes of the PIGEs, the shape of the trajectory of the rotary axes is close to circular. In a similar way to [21], least squares fitting of circles are thus used to calculate the position errors [28]. Further, for a constant feed rate, the points are considered uniformly distributed, and we may set

$$\theta_i = \frac{i}{N} \cdot \Theta \tag{2}$$

$$Y_i = (R_n + \delta_i) \cdot \cos(\theta_i + \delta_e) \tag{3}$$

$$Z_i = (R_n + \delta_i) \cdot \sin(\theta_i + \delta_e) \tag{4}$$

where Y_i and Z_i are the Y and Z coordinates of the ith point, $P_i = (X_i, Y_i, Z_i)$, lying on the DBB table ball trajectory. δ_i and θ_i are the captured DBB length variations and the rotational angle of the ith point respectively. N is the total number of captured points. Θ is the total angle of rotation. The nominal length of the DBB is represented by R_n; Y_i and Z_i are the coordinates of the table ball centre respectively.

The position errors are then determined from:

$$(y - E_{Y0A})^2 + (z - E_{Z0A})^2 = R^2 \tag{5}$$

where y and z are the Y and Z components of the points lying on the fit circle respectively. E_{Y0A} and E_{Z0A} are the position errors in Y- and Z-axes directions respectively. R is the radius of the least squares fitted circle. Further, the distance between the point P_i and the rotation centre d_i can be calculated from:

$$(Y_i - E_{Y0A})^2 + (Z_i - E_{Z0A})^2 = d_i^2. \tag{6}$$

Least Squares Fitting minimises the sum of the differences between the distance d_i and the fitting radius R. Therefore let

$$f(a, b, c) = \sum_{i=0}^{N} (d_i^2 - R^2)^2 = \sum_{i=0}^{N} (Y_i^2 + Z_i^2 + aY_i + bZ_i + c)^2 \tag{7}$$

where

$$a = -2 \cdot E_{Y0A}$$

$$b = -2 \cdot E_{Z0A}$$

$$c = E_{Y0A}^2 + E_{Z0A}^2 - R^2.$$

To obtain the minimum value of the above equation, total derivatives of $f(a, b, c)$ with respect to a, b and c are given, which can be written in matrix form

$$\begin{bmatrix} \sum_{i=0}^{N} Y_i^2 & \sum_{i=0}^{N} Y_i Z_i & \sum_{i=0}^{N} Y_i \\ \sum_{i=0}^{N} Y_i Z_i & \sum_{i=0}^{N} Z_i^2 & \sum_{i=0}^{N} Z_i \\ \sum_{i=0}^{N} Y_i & \sum_{i=0}^{N} Z_i & N \end{bmatrix} \begin{bmatrix} a \\ b \\ c \end{bmatrix} = \begin{bmatrix} \sum_{i=0}^{N} (Y_i^3 + Y_i Z_i^2) \\ \sum_{i=0}^{N} (Y_i^2 Z_i + Z_i^3) \\ \sum_{i=0}^{N} (Y_i^2 + Z_i^2) \end{bmatrix}. \tag{8}$$

Expressing P_i in terms of error coordinate $\{E\}$

$${}^E P_i = [0 \quad Y_i \quad Z_i \quad 0]^T \tag{9}$$

thus misalignment-compensation vectors ${}^A P_i$ with respect to the local coordinate $\{O'\}$ are given by

$${}^{O'} P_i = {}^{O'}_E T \cdot {}^E P_i \tag{10}$$

where

$${}^{O'}_E T = \begin{bmatrix} 1 & 0 & 0 & 0 \\ 0 & \cos\alpha & -\sin\alpha & E_{Y0A} \\ 0 & \sin\alpha & \cos\alpha & E_{Z0A} \\ 0 & 0 & 0 & 1 \end{bmatrix}.$$

${}^{O'}_E T$ is the transformation matrix from $\{E\}$ to $\{O'\}$, E_{Y0A} and E_{Z0A} are the Y and Z coordinate components of the vector from the origin of $\{E\}$ pointing to the origin of $\{O'\}$ respectively. They are also the position errors in the Y and Z directions of the A-axis, α is the rotational angle from $\{E\}$ to $\{O'\}$.

3.4. Tests with an extension bar

For the purpose of making the orientation errors evident, a different configuration is applied. As shown in Fig. 4(b), an extension bar (50 mm) is added to the DBB in order to amplify the effect of the orientation errors. The X-axis is driven in the negative direction to fit the longer length without moving the table pivot. An exaggerated diagram to illustrate the error is given in Fig. 6.

The position errors calculated in the first step in Fig. 4 can be denoted as the length $O'P$ in Fig. 6, where the point O' is the ideal rotation centre whilst the point P is the offset centre due to the position errors. In the second step with the extension bar, the spindle tool cup centre is shifted to S'. In order to transfer the captured lengths of the DBB to the bottom plane of the cone, a normal line passing through S' is made, having an intersection point E with the bottom surface formed by EP_i. In the triangle $\triangle S'P_iE$,

$$S'P_i^2 = S'E^2 + EP_i^2. \tag{11}$$

Expressing L_i in terms of the radius of the bottom circle of the cone EP_i, fitted using least squares, the distance EP can be obtained from Eqs. (12) to (14).

$$(y - Y_{EP})^2 + (z - Z_{EP})^2 = R_f^2 \tag{12}$$

where y and z are the Y and Z components of the points lying on the fit circle respectively. Y_{EP} and Z_{EP} are the Y and Z components of EP respectively. R_f is the radius of the least squares fitted circle.
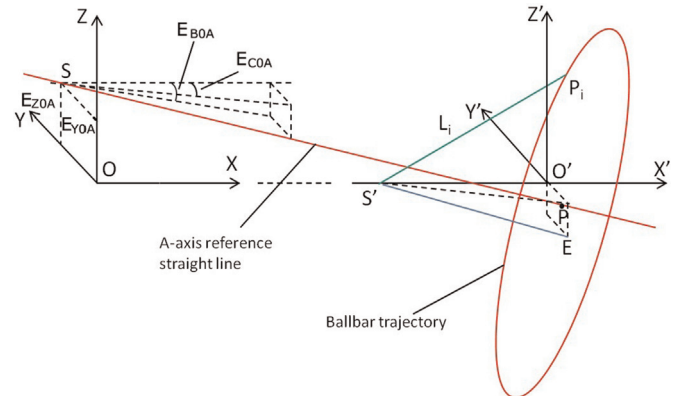

Fig. 6. An exaggerated schematic view highlighting the PIGEs of the A-axis.

$$(Y_i - Y_{EP})^2 + (Z_i - Z_{EP})^2 = EP_i^2 \qquad (13)$$

$$g(m, n, p) = \sum_{i=0}^{N} (EP_i^2 - R^2)^2 = \sum_{i=0}^{N} (Y_i^2 + Z_i^2 + mY_i + nZ_i + p)^2 \qquad (14)$$

where

$$m = -2 \cdot Y_{EP}$$

$$n = -2 \cdot Z_{EP}$$

$$p = Y_{EP}^2 + Z_{EP}^2 - R_f^2.$$

Finally equate the total derivatives of $g(m, n, p)$ with respect to m, n and p to 0. Thus Y_{EP} and Z_{EP} are given as

$$Y_{EP} = -\frac{m}{2} \qquad (15)$$

$$Z_{EP} = -\frac{n}{2} \qquad (16)$$

$$R_f = \frac{1}{2}\sqrt{m^2 + n^2 - 4p}. \qquad (17)$$

Since SP and $S'E$ are normal to the bottom plane, the orientation errors of $S'E$ are the same as those errors of SP. Therefore the orientation errors E_{B0A} and E_{C0A} can be calculated as

$$E_{B0A} = \tan^{-1}\frac{Z_{O'E}}{\|S'O'\|}; \qquad (18)$$

$$E_{C0A} = \tan^{-1}\frac{Y_{O'E}}{\|S'O'\|}. \qquad (19)$$

where $Y_{O'E}$ and $Z_{O'E}$ are the Y and Z components of $O'E$ respectively. Here the length $O'E$ is approximated as $EP + PO'$. Although EP and PO' are not in the same plane, $EP + PO'$ is used instead of $O'E$, since $O'E$ cannot be determined without knowing E_{B0A} and E_{C0A}. The resulting difference of the substitution Δ can be determined from:

$$\Delta = (EP + PO') - O'E = PO'\left(\frac{1}{\cos E_{B0A}}\cos E_{C0A} - 1\right). \qquad (20)$$

Tests without the extension bar showed that E_{B0A} and E_{C0A} are smaller than $1°$ (Assuming the centre offsets captured in step 1 and 3 are all due to orientation PIGEs, and the results of the orientation PIGEs are smaller than $1°$). This suggests that Δ is less than 10^{-8} mm which is small enough to neglect.

4. Experimental validation

The proposed method is tested on a Hermle C600U five-axis machine tool, whose structure is shown in Fig. 1. An overshoot angle for all tests is given to stabilise the machine movement (Table 1) [17].

Before every test the machine tool is warmed up for 20 min according to the standard warming-up procedure recommended in [6]. The four steps of the tests take approximately 30 min including the set-up process.

Figures before and after compensation of the A- and C-axes are given in Figs. 7 and 8 to show the effectiveness of the proposed method. After the diagnosed PIGEs are compensated to the target axes, residual errors still exist in the A- and C-axes. However the value of the remaining errors is within tolerance (1 μm), shown in Fig. 9 for both axes. Tests with different feed rates were carried out to identify the remaining error sources. It has been determined that with an increasing feed rate, the residual errors increase.
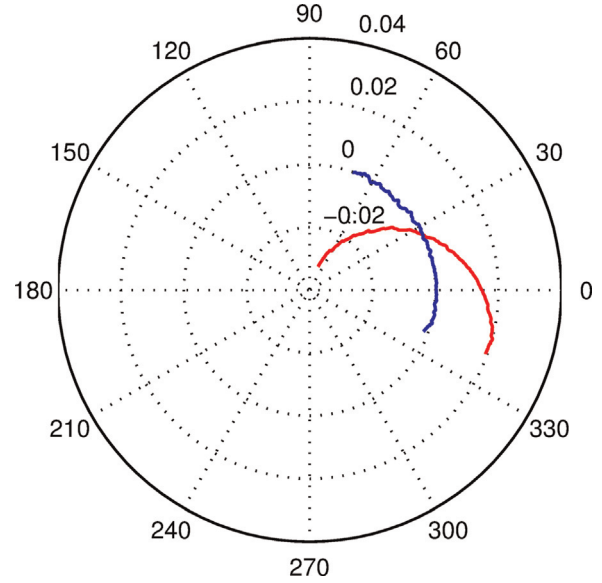

Fig. 7. *A*-axis test result with (blue) and without compensation (red) (mm). (For interpretation of the references to color in this figure caption, the reader is referred to the web version of this article.)

Fig. 8. *C*-axis test result with (blue) and without compensation (red) (mm). (For interpretation of the references to color in this figure caption, the reader is referred to the web version of this article.)
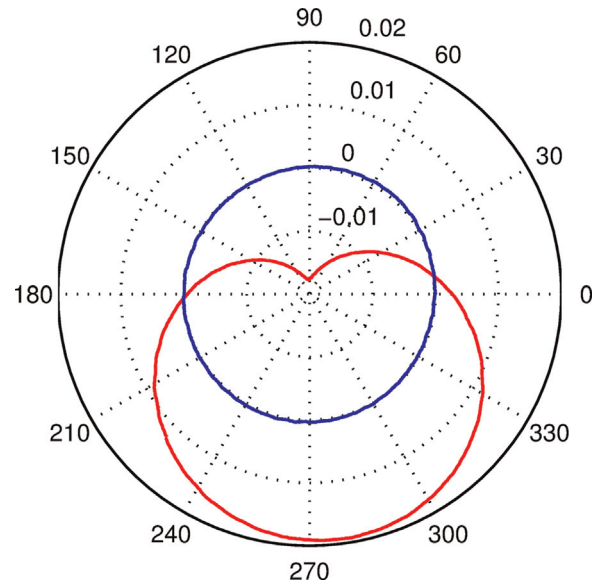
Since the geometric errors are not effected by the feed rate, the residual errors are likely to be caused by dynamic errors, as those are feed rate influenced [4].

The test was repeated 10 times until the repeatability was within the tolerance (1 μm for position PIGEs and $1''$ for orientation PIGEs). Averages and standard deviations of all testing results are calculated based on the repeatability tests, given in Tables 2 and 3. Among those PIGEs, E_{Y0C} and E_{A0C} are fairly large compared to the other errors. Nonetheless they can also be compensated with the tested values and the compensated results (Fig. 9) are within tolerances. Therefore the reason of E_{Y0C} and E_{A0C} being relatively large might be due to the worn condition of the C-axis.
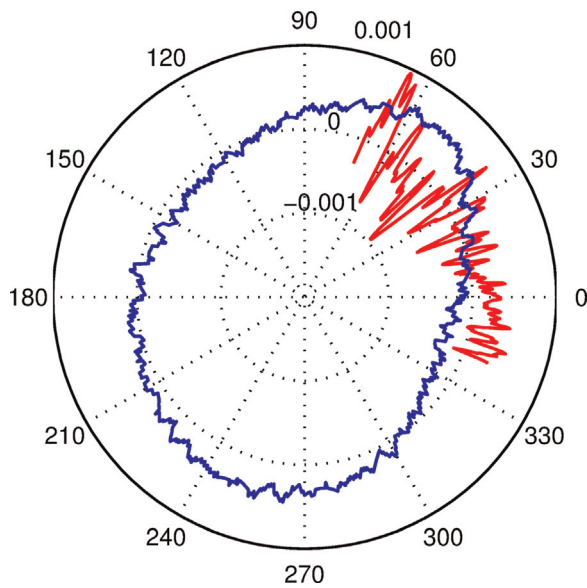
Fig. 9. Residual error of the A- (red) and C-axis (blue) test with compensation (mm). (For interpretation of the references to color in this figure caption, the reader is referred to the web version of this article.)

Table 1
Specification of DBB test.

Parameters	Value
Nominal length R_n (mm)	100.0000
Calibrated length R_c (no extension bar) (mm)	99.9881
Calibrated length R_e (with extension bar) (mm)	149.9946
Overshooting angle (degree) (C-axis)	45°
Overshooting angle (degree) (A-axis)	2°
Testing feed rate F (mm/min)	500

Table 2
Test results for position PIGEs.

Parameters	Average (mm)	Standard deviation (mm)
E_{Y0A}	0.0342	0.00008
E_{Z0A}	−0.0353	0.00037
E_{X0C}	0.0013	0.00015
E_{Y0C}	−0.0525	0.0006

Table 3
Test results for orientation PIGEs.

Parameters	Average (″)	Standard deviation (″)
E_{B0A}	6.62	0.557
E_{C0A}	1.89	0.388
E_{A0C}	−22.32	0.489
E_{B0C}	−3.75	0.527

5. Conclusions

This study presents a new procedure using a DBB to identify and characterise the PIGEs of a five-axis machine tool using new testing paths in the A- and C-axes. The four steps of the procedure consists of tests with and without the use of an extension bar for both the A- and C-axes. Since the C-axis rotary table is designed on top of the A-axis tilting table, the tests start from the A-axis measurement. The first testing step, without an extension bar, is to determine the position errors. Then using a 50 mm extension bar the orientation errors can be obtained. Similar steps are used for

C-axis tests after compensating for the A-axis errors. The procedure is then validated using a five-axis machine tool.

By controlling the rotary axis individually, the analysis of PIGEs is simplified since the result only reflects the error condition of the axis under test. Other advantages of the proposed method are that it requires no additional fixturing, and is applicable to other types of five-axis machine tools with rotary axes in the workpiece side. This proposed method is effective and can be considered as a form of regular acceptance test of machine accuracy.

Acknowledgements

References

[1] H. Schwenke, W. Knapp, H. Haitjema, A. Weckenmann, R. Schmitt, F. Delbressine, Geometric error measurement and compensation of machines—an update, CIRP Ann. Manuf. Technol. 57 (2) (2008) 660–675.
[2] R. Ramesh, M.A. Mannan, A.N. Poo, Error compensation in machine tools—review: Part I: geometric, cutting-force induced and fixture-dependent errors, Int. J. Mach. Tools Manuf. 40 (9) (2000) 1235–1256.
[3] ISO/DIS10791-6, Test code for machine tools-Part 1: geometric accuracy of machines operating under no-load or quasi-static Conditions, ISO, 2012.
[4] W.T. Lei, I.M. Paung, C.C. Yu, Total ballbar dynamic tests for five-axis CNC machine tools, Int. J. Mach. Tools Manuf. 49 (6) (2009) 488–499.
[5] S. Ibaraki, W. Knapp, Indirect measurement of volumetric accuracy for three-axis and five-axis machine tools: a review, Int. J. Autom. Technol. 6 (2) (2012) 110–124.
[6] ISO230-1, Test code for machine tools-Part 1: geometric accuracy of machines operating under no-load or quasi-static conditions, ISO, 2012.
[7] J.P. Heui, S.K. Young, H.M. Joon, A new technique for volumetric error assessment of CNC machine tools incorporating ball bar measurement and 3d volumetric error model, Int. J. Mach. Tools Manuf. 37 (11) (1997) 1583–1596.
[8] K.I. Lee, S.H. Yang, Robust measurement method and uncertainty analysis for position-independent geometric errors of a rotary axis using a double ball-bar, Int. J. Precis. Eng. Manuf. 14 (2) (2013) 231–239.
[9] Y. Abbaszadeh-Mir, J.R.R. Mayer, G. Cloutier, C. Fortin, Theory and simulation for the identification of the link geometric errors for a five-axis machine tool using a telescoping magnetic ball-bar, Int. J. Prod. Res. 40 (18) (2002) 4781–4797.
[10] S.R. Park, S.H. Yang, Design of a 5-axis machine tool considering geometric errors, Int. J. Mod. Phys. B 24 (15–16) (2010) 2484–2489.
[11] K.I. Lee, D.M. Lee, S.H. Yang, Parametric modeling and estimation of geometric errors for a rotary axis using double ball-bar, Int. J. Adv. Manuf. Technol. 62 (5–8) (2012) 741–750.
[12] J.M. Lai, J.S. Liao, W.H. Chieng, Modeling and analysis of nonlinear guideway for double-ball bar (DBB) measurement and diagnosis, Int. J. Mach. Tools Manuf. 37 (5) (1997) 687–707.
[13] J.P. Heui, S.K. Young, H.M. Joon, A new technique for volumetric error assessment of CNC machine tools incorporating ball bar measurement and 3d volumetric error model, Int. J. Mach. Tools Manuf. 37 (11) (1997) 1583–1596.
[14] B. Bringmann, W. Knapp, Machine tool calibration: geometric test uncertainty depends on machine tool performance, Precis. Eng. 33 (4) (2009) 524–529.
[15] ⟨http://www.renishaw.com/en/xr20-w-rotary-axis-calibrator-15763⟩.
[16] Renishw plc., Quick start guide: AxiSet Check-Up, 2011.
[17] Renishw plc., Renishaw QC20-W Ballbar system help menu, 2009.
[18] M. Tsutsumi, A. Saito, Identification and compensation of systematic deviations particular to 5-axis machining centers, Int. J. Mach. Tools Manuf. 43 (8) (2003) 771–780.
[19] K. Dassanayake, M. Tsutsumi, A. Saito, A strategy for identifying static deviations in universal spindle head type multi-axis machining centers, Int. J. Mach. Tools Manuf. 46 (10) (2006) 1097–1106.
[20] S. Ibaraki, Y. Kakino, T. Akai, N. Takayama, I. Yamaji, K. Ogawa, Identification of motion error sources on five-axis machine tools by ball-bar measurements (1st report)-classification of motion error components and development of the modified ball bar device (DBB5), J. Jpn. Soc. Precis. Eng. 76 (3) (2010) 333–337.
[21] K.I. Lee, S.H. Yang, Measurement and verification of position-independent geometric errors of a five-axis machine tool using a double ball-bar, Int. J. Mach. Tools Manuf. 70 (0) (2013) 45–52.
[22] W.T. Lei, M.P. Sung, W.L. Liu, Y.C. Chuang, Double ballbar test for the rotary axes of five-axis CNC machine tools, Int. J. Mach. Tools Manuf. 47 (2) (2007) 273–285.

[23] NAS979, Uniform Cutting Tests-NAS Series, Metal Cutting Equipment Specifications, AIA, 1969.

[24] Y. Ihara, Ball bar measurement on machine tools with rotary axes, Int. J. Autom. Technol. 6 (2) (2012) 180–187.

[25] N. Kato, M. Tsutsumi, R. Sato, Analysis of circular trajectory equivalent to cone-frustum milling in five-axis machining centers using motion simulator, Int. J. Mach. Tools Manuf. 64 (1) (2013) 1–11.

[26] C. Hong, S. Ibaraki, A. Matsubara, Influence of position-dependent geometric errors of rotary axes on a machining test of cone frustum by five-axis machine tools, Precis. Eng. 35 (1) (2010) 1–11.

[27] E.L.J. Bohez, Five-axis milling machine tool kinematic chain design and analysis, Int. J. Mach. Tools Manuf. 42 (4) (2002) 505–520.

[28] S.H.H. Zargarbashi, J.R.R. Mayer, A model based method for centering double ball bar test results preventing fictitious ovalization effects, Int. J. Mach. Tools Manuf. 45 (10) (2005) 1132–1139.